1994

New solutions for the propagation of long water waves over variable depth

Yinglong Zhang
University of Wollongong

Song-Ping Zhu
University of Wollongong, spz@uow.edu.au

New solutions for the propagation of long water waves over variable depth

Abstract

Based on the linearized long-wave equation, two new analytical solutions are obtained respectively for the propagation of long surface gravity waves around a conical island and over a paraboloidal shoal. Having been intensively studied during the last two decades, these two problems have practical significance and are physically revealing for wave propagation over variable water depth. The newly derived analytical solutions are compared with several previously obtained numerical solutions and the accuracy of those numerical solutions is discussed. The analytical method has the potential to be used to find solutions for wave propagation over more natural bottom topographies.

Keywords

over, long, water, depth, waves, propagation, solutions, variable

Disciplines

Engineering | Science and Technology Studies

Publication Details

Zhang, Y. & Zhu, S. (1994). New solutions for the propagation of long water waves over variable depth. Journal of Fluid Mechanics, 278 391-406.

J. Fluid Mech. (1994), *vol.* 278, *pp.* 391–406

New solutions for the propagation of long water waves over variable depth

By YINGLONG ZHANG AND SONGPING ZHU
Department of Mathematics, The University of Wollongong, Wollongong, NSW 2500, Australia

(Received 24 November 1993 and in revised form 16 June 1994)

Based on the linearized long-wave equation, two new analytical solutions are obtained respectively for the propagation of long surface gravity waves around a conical island and over a paraboloidal shoal. Having been intensively studied during the last two decades, these two problems have practical significance and are physically revealing for wave propagation over variable water depth. The newly derived analytical solutions are compared with several previously obtained numerical solutions and the accuracy of those numerical solutions is discussed. The analytical method has the potential to be used to find solutions for wave propagation over more natural bottom topographies.

1. Introduction

When a tsunami (usually of very long wavelength) is propagating over waters of variable depth, it may be greatly amplified due to the variation of water depth. Among various problems on wave propagation over variable water depth, two well-known ones have been most intensively studied since the early 1970s due to their physical and practical significance. However, to the authors' knowledge, the analytical solutions of these two problems have not yet been found. The two problems are:

(i) Scattering of waves by a conical island. It has been studied by, among many others, Lautenbacher (1970), who derived an integral equation for this problem and then solved it numerically, Smith & Sprinks (1975), who used this problem as an example to demonstrate the mild-slope equation and compared their results with Lautenbacher's (1970), and Shen & Meyer (1968), who discussed edge waves around conical islands which is an analogue of the edge waves occurring in one-dimensional sloping beaches (Eckart 1951). Islands of this shape may represent some realistic ones, such as the Hawaii Islands studied by Lautenbacher (1970) and the gravity platforms in the Arctic studied by Sarpkaya & Isaacson (1981). It is of great concern to ocean engineers how large wave runs-ups can be built up at the coastline of an island, as a consequence of refractive focusing or resonance of virtually trapped waves (Eckart 1950; Longuet-Higgins 1967).

(ii) Propagation of waves over a submerged paraboloidal shoal. Upon introducing the mild-slope equation, Berkhoff (1972) gave a first numerical solution for this problem. Since then, similar problems have been studied by a number of authors, e.g. Ito & Tanimoto (1972), who additionally conducted some laboratory experiments, Bettess & Zienkiewitz (1977), who found that one of their solutions for long waves was quite different from Berkhoff's (1972) in a certain part of the wave field, Radder (1979), who applied the parabolic equation method to study short waves, and Kirby & Dalrymple (1983), who used a nonlinear model to study wave-jump in the vicinity of caustics.

This paper is aimed at demonstrating a widely applicable approach to analytically

solve the linearized long-wave equation, for axisymmetric sea bottom topographies. The analytical solutions to this simplified equation are not only useful checks on the results from more complicated models in long-wave range, but also of great practical significance since they provide realistic simulations of long waves occurring in many circumstances (Mei 1989); diffraction, refraction as well as other physical properties can be better understood. Therefore, the new analytical solutions are a significant supplement to the existing ones (see e.g. a classical solution by Homma 1950, and more recently, an analytical solution by Zhu & Zhang 1994).

In the next section, such an approach is outlined for general cases of axisymmetric sea bottom topographies. Then, as examples to demonstrate its usefulness, two new analytical solutions are shown in §§3 and 4 respectively for the propagation of long surface gravity waves around a conical island and over a paraboloidal shoal. Our analytical solutions are compared with several previously obtained numerical solutions and the accuracy associated with these numerical solutions is discussed. The main findings in this paper are briefly summarized in the last section.

2. Mathematical theory and solution technique

In the following discussion, the ocean water is assumed to be inviscid and incompressible. Let the origin of a Cartesian coordinate system $O(x, y, z)$ be placed in the mean water surface and the z-coordinate increases vertically upwards. A train of plane monochromatic waves of small wave steepness is propagating over waters of variable depth $h(x, y)$. Furthermore, we assume that the flow associated with the wave motion is irrotational and the wavelength is long compared to the water depth. Thus there exists a velocity potential $\Phi(x, y, z, \tau)$. Upon assuming the fluid motion to be time harmonic and linearizing the problem, the time-independent part of the water elevation $\eta(x, y)$ satisfies the long-wave equation

$$\nabla \cdot (h \nabla \eta) + \frac{\omega^2}{g} \eta = 0, \tag{1}$$

where ∇ is the horizontal gradient operator, ω is the angular frequency and g is the gravitational acceleration. Time-dependent variables (such as the water elevation and velocity potential) are all proportional to $\exp(-\mathrm{i}\omega\tau)$, where $\mathrm{i} = \sqrt{-1}$ and τ is the time variable.

The governing differential system also includes some no-flow conditions along solid boundaries if necessary and Sommerfeld's radiation condition to ensure the energy associated with the scattered waves propagates towards infinity without being reflected back.

With a horizontal characteristic lengthscale, L_s, being adopted to non-dimensionalize any horizontal variable with lengthscale, L, and the incident wave amplitude, A, being adopted to non-dimensionalize any vertical variable with lengthscale (such as η), i.e. by letting

$$L' = L/L_s, \quad k' = kL_s, \quad \eta' = \eta/A, \tag{2}$$

the dimensionless version of (1) now reads

$$\nabla \cdot (h \nabla \eta) + \mu^2 \eta = 0, \tag{3}$$

where $\mu^2 = \omega^2 L_s/g$. In (3) and hereafter, all the primes denoting dimensionless quantities are dropped for simplicity.

If the sea-bottom contours are axisymmetric with respect to the z-axis, it is convenient to adopt a cylindrical coordinate system (r, θ, z) with $x = r\cos\theta$ and

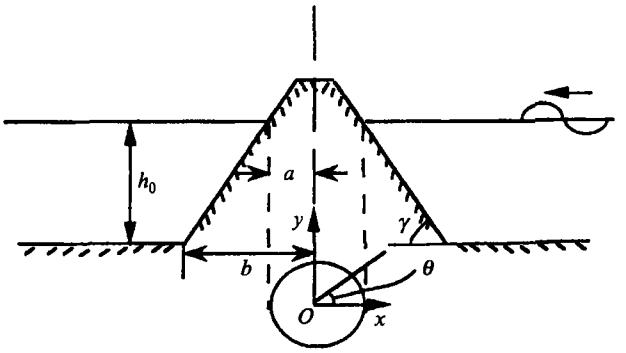

FIGURE 1. A definition sketch: plane long waves scattered by a conical island.

$y = r\sin\theta$. In this special case, h is a function of r only and a solution to (3) can be constructed via the separation of variables as

$$\eta = \sum_{n=0}^{\infty} R_n(r)\cos n\theta, \tag{4}$$

with $R_n(r)$ satisfying

$$hr^2R_n'' + (r^2h' + hr)R_n' + (\mu^2r^2 - n^2h)R_n = 0, \tag{5}$$

in which the primes denote derivatives with respect to r. Equation (5) is a second-order ordinary differential equation with variable coefficients; in two special cases where h is of the form $h = lr^{\alpha}$ with l being a constant and α being equal to 2 and 1 respectively, solutions to (5) have been found by Homma (1950) (for a circular island mounted on a paraboloidal shoal) and by Zhu & Zhang (1994) (for a circular island mounted on a conical shoal) in terms of simple elementary or Bessel functions.

For a general axisymmetric bottom topography with h being a polynomial function of r (or able to be expanded in a series of polynomial functions), a series solution (Taylor series or Frobenius-type series) can be attempted. However, one may encounter great difficulty in such an attempt if the domain of interest contains some points at which the series solution does not converge. According to Frobenius' theory (Spiegel 1981), if $R_n(r)$ is expanded at a non-singular or regular singular point $r = r_1$, the series solution and its derivatives converge for all complex r such that $|r - r_1| < R$ where R is the distance from $r = r_1$ to the nearest singularity (other than $r = r_1$). Therefore a crucial step is to find an expansion point (either non-singular or regular singular) such that the convergent circle encompasses the domain of interest. To achieve this, suitable mappings can be employed; their search, though, sometimes can be quite difficult. Furthermore, a good choice of expansion point may also substantially simplify the solution procedure. We shall now demonstrate the above qualitative outline of the general approach utilizing two examples.

3. Scattering of plane long waves by conical islands

Let us consider a train of plane long waves propagating along the negative x-direction and being scattered by a conical island standing in an open sea of constant depth (see figure 1). If the characteristic lengthscale L_s (see (2)) is chosen as the radius of the island at the free surface, a, then in the region with variable water depth ($1 \leqslant r \leqslant b/a$) we have $h = \gamma(r-1)$ (see figure 1) and therefore (5) becomes

$$r^2(r-1)R_n'' + r(2r-1)R_n' + (\nu^2r^2 - n^2r + n^2)R_n = 0, \tag{6}$$

where $\nu^2 = \mu^2/\gamma = k_0^2(b/a-1)$, and k_0 is the dimensionless wavenumber in the constant-depth region $r \geqslant b/a$.

For a similar island, Zhu & Zhang (1994) found an analytical solution in terms of Bessel functions of fractional order. However, to avoid difficulties associated with the singularity introduced due to the water depth being zero at the coastline, they placed a vertical wall along the coastline, which is a common approach adopted by many authors (e.g. Homma 1950; Vastano & Reid 1966; Christiansen 1975). With no wall being located at the coastline and the water depth being assumed to be zero there, searching for an analytical solution becomes much more difficult.

Now, if we assume that the water depth at the coastline is zero and the waves are not steep enough to break, an appropriate boundary condition to be imposed along the coastline of the island $r = 1$ (see Mei 1989) is

$$\lim_{r\to 1} h\frac{\partial \zeta}{\partial r} = 0,$$

which amounts to

$$\lim_{r\to 1} h\frac{\mathrm{d}R_n}{\mathrm{d}r} = 0. \tag{7}$$

To utilize this boundary condition conveniently, we choose the expansion point at $r = 1$, which is a regular singular point of (6). From Frobenius' theory, Frobenius' series solution converges for $|r-1| < 1$. On the other hand, the domain under concern (the region with variable water depth) is $1 \leqslant r \leqslant b/a$, which may not lie in the convergent region of the series. To ensure the domain of interest lies within the convergent region, a mapping

$$t = 1-1/r, \tag{8}$$

is constructed. Under this transformation, (6) becomes

$$t(1-t)^3\frac{\mathrm{d}^2R_n}{\mathrm{d}t^2}+(1-t)^3\frac{\mathrm{d}R_n}{\mathrm{d}t}+(n^2t^2-n^2t+\nu^2)R_n = 0, \tag{9}$$

and the domain of interest is now mapped into $0 \leqslant t \leqslant 1-a/b$. It should also be noticed that the original expansion point $r = 1$ has been mapped onto $t = 0$, which is a regular singular point of (9). From Frobenius' theory, a series solution of the form

$$R_n(t) = \sum_{m=0}^{\infty} a_{m,n}\, t^{m+c}, \tag{10}$$

with $a_{0,n}$ being unity and the constant c to be determined by the so-called indicial equation, converges for $|t| < 1$. On the other hand, since $1-a/b < 1$, the convergent region of the series solution now contains the mapped domain of interest as a subdomain. A series solution which converges throughout the region of variable water depth has been successfully constructed. After substituting (10) into (9) and collecting terms of the same order of t, we have

$$c = 0 \text{ (double repeated roots)}, \tag{11}$$

$$a_{1,n} = -\nu^2, \tag{12}$$

$$a_{2,n} = \tfrac{1}{4}(\nu^4-3\nu^2+n^2), \tag{13}$$

$$a_{m+3,n} = \frac{[3(m+2)^2-\nu^2]a_{m+2,n}-[3(m+1)^2-n^2]a_{m+1,n}+(m^2-n^2)a_{m,n}}{(m+3)^2},$$

$$m = 0, 1, 2, \ldots. \tag{14}$$

Since the indicial equation has double repeated roots, there is only one particular solution in the form of the Frobenius' series (10). Another linearly independent particular solution contains logarithmic terms (Spiegel 1981) which clearly violate the boundary condition (7), and therefore should be excluded from the final solution. Consequently, in the region with variable water depth, the general solution reads

$$R_n(r) = A_n \sum_{m=0}^{\infty} a_{m,n}(1-r^{-1})^m \equiv A_n \bar{R}_n(r), \tag{15}$$

and from (4), the water elevation is given by

$$\eta_1(r,\theta) = \sum_{n=0}^{\infty} A_n \bar{R}_n(r)\cos n\theta, \tag{16}$$

in which the constants A_n are yet to be determined.

In the constant-depth region ($r \geqslant b/a$), the solution is well-known (MacCamy & Fuchs 1954) and can be written as

$$\eta_2(r,\theta) = \eta_2^I + \eta_2^S = \sum_{n=0}^{\infty} [(-\mathrm{i})^n \epsilon_n J_n(k_0 r) + C_n H_n^{(2)}(k_0 r)]\cos n\theta, \tag{17}$$

in which η_2^I, η_2^S are the incident and scattered waves respectively, J_n is the Bessel function of the first kind of order n, $H_n^{(2)}$ is the Hankel function of the second kind of order n, and ϵ_n is the Jacobi symbol ($\epsilon_n = 1$ for $n = 0$ and $\epsilon_n = 2$ for $n > 0$). The constant coefficients C_n in (17) are also to be determined.

The solutions in the two regions must be matched on the common boundary $r = b/a \equiv r_0$ to ensure the continuity of wave heights and flow fluxes across it, i.e.

$$\eta_1 = \eta_2, \quad \frac{\partial \eta_1}{\partial r} = \frac{\partial \eta_2}{\partial r}. \tag{18}$$

Therefore from (16)–(18), the coefficients A_n and C_n can be determined as

$$A_n = -\frac{2\epsilon_n(-\mathrm{i})^{n+1}}{\pi r_0 \Delta}, \tag{19}$$

$$C_n = \Delta_1/\Delta, \tag{20}$$

$$\Delta_1 = (-\mathrm{i})^n \epsilon_n \begin{vmatrix} \bar{R}_n(r_0) & J_n(k_0 r_0) \\ \bar{R}_n'(r_0) & k_0 J_n'(k_0 r_0) \end{vmatrix}, \tag{21}$$

$$\Delta = \begin{vmatrix} \bar{R}_n(r_0) & -H_n^{(2)}(k_0 r_0) \\ \bar{R}_n'(r_0) & -k_0 H_n^{(2)\prime}(k_0 r_0) \end{vmatrix}, \tag{22}$$

in which $\bar{R}_n(r)$ was defined in (15), and the primes denote derivatives with respect to the arguments. The water elevation at the coastline of the island $r = 1$ is

$$[\zeta_1]_{r=1} = [\eta_1]_{r=1}\exp(-\mathrm{i}\omega\tau) = \exp(-\mathrm{i}\omega\tau)\sum_{n=0}^{\infty} A_n \cos n\theta, \tag{23}$$

and the normal velocity there is

$$u_r = -\frac{\mathrm{i}g}{\omega}\left[\frac{\partial \zeta_1}{\partial r}\right]_{r=1} = \chi \exp(-\mathrm{i}\omega\tau)\sum_{n=0}^{\infty} A_n \cos n\theta, \tag{24}$$

where $\chi = -\mathrm{i}g\omega^{-1}a_{1,n} = \mathrm{i}\omega a\gamma^{-1}$. Comparing (23) with (24) reveals

$$u_r = \chi[\zeta_1]_{r=1}, \tag{25}$$

which can be recovered directly from the long-wave equation (3) with $h \to 0$ and is a well-known result. Equation (25) indicates that the normal velocity is proportional to the wave run-up at the coastline of the island. Unlike the case that an island is surrounded by a vertical wall, where the normal velocity vanishes, the normal velocity in the case being studied here is usually very large (especially for large value of χ), because the wave run-up at the coastline is usually very large. This will be demonstrated quantitatively in the following discussion.

Zhu & Zhang (1994) showed, in their analytical solution for long waves scattered by a circular island mounted on a conical shoal, that the wave amplitudes and phase are only dependent on a dimensionless geometric parameter b/a and a dimensionless wavelength λ_0/b (λ_0 is the wavelength of incident waves). For the problem discussed in this section, one can reach exactly the same conclusion: that is to say, the final solution only depends on the values of b/a and λ_0/b. However, fixed values of b/a and λ_0/b can lead to infinitely many combinations of the water depth h_0 and wave period T.

The same problem studied here was solved numerically by Lautenbacher (1970), who used the conical island to represent three individual Hawaiian islands (Hawaii, Oahu and Small). He recast the problem into an integral equation which was then solved numerically. Since double integrals were involved in his calculation, the approach seems to be very laborious. Smith & Sprinks (1975) also used the same example to demonstrate the mild-slope equation but only presented the results for the long-wave equation. They obtained an asymptotic solution near the coastline of the island and calculated the far-field solution via an integral equation method. Their method is a little simpler than Lautenbacher's (1970) since only single integrals were involved in the calculation. However, it suffers from a drawback that the location of the 'far field' is somehow ambiguous. Furthermore, only the first seven terms ('modes') in the asymptotic expansion were calculated, which may not be adequate.

The numerical results calculated from the analytical solution presented in this paper were compared with those shown in the papers by Lautenbacher and by Smith & Sprinks. A computer program was written to evaluate the double-series solution (16) (the power series $\bar{R}_n(r)$ and the Fourier series (16)) numerically. To calculate the power series $\bar{R}_n(r)$, terms were summed till convergent results were obtained. It should be emphasized here that through the carefully constructed mapping (8), the convergence of our series solution (16) is guaranteed. As far as the speed of convergence is concerned, for larger values of r, $\bar{R}_n(r)$ converges less rapidly. But even for the most difficult numerical calculation presented in this paper (when $r = b/a$), converged results (within an error of 0.00000001 %) were obtained with no more than 200 terms required at the expense of virtually zero CPU time on a SUN 4/470 Sparc Server. On the other hand, the Fourier series (16) converges much faster; no more than twenty terms ('modes') was found to be sufficient for all of the numerical calculations presented in this paper. The overall numerical efficiency is reflected by the fact that it took only 24 CPU minutes to calculate the relative amplitudes and the wave phases (presented in figures 3 and 4 respectively) at about 10000 points in the physical domain.

Shown in figure 2(*a–c*) are the dimensionless maximum wave amplifications around the coastline of the island, obtained respectively from the analytical solution, Lautenbacher's integral equation solution and Smith & Sprinks' asymptotic solution. For smaller b/a (such as Hawaii and Oahu), Lautenbacher's results exhibit a reasonable agreement with the analytical solution whereas large discrepancies were found in most cases between the analytical solution and Smith & Sprinks' solution. The discrepancies are thought to be the consequence of the insufficient number of terms

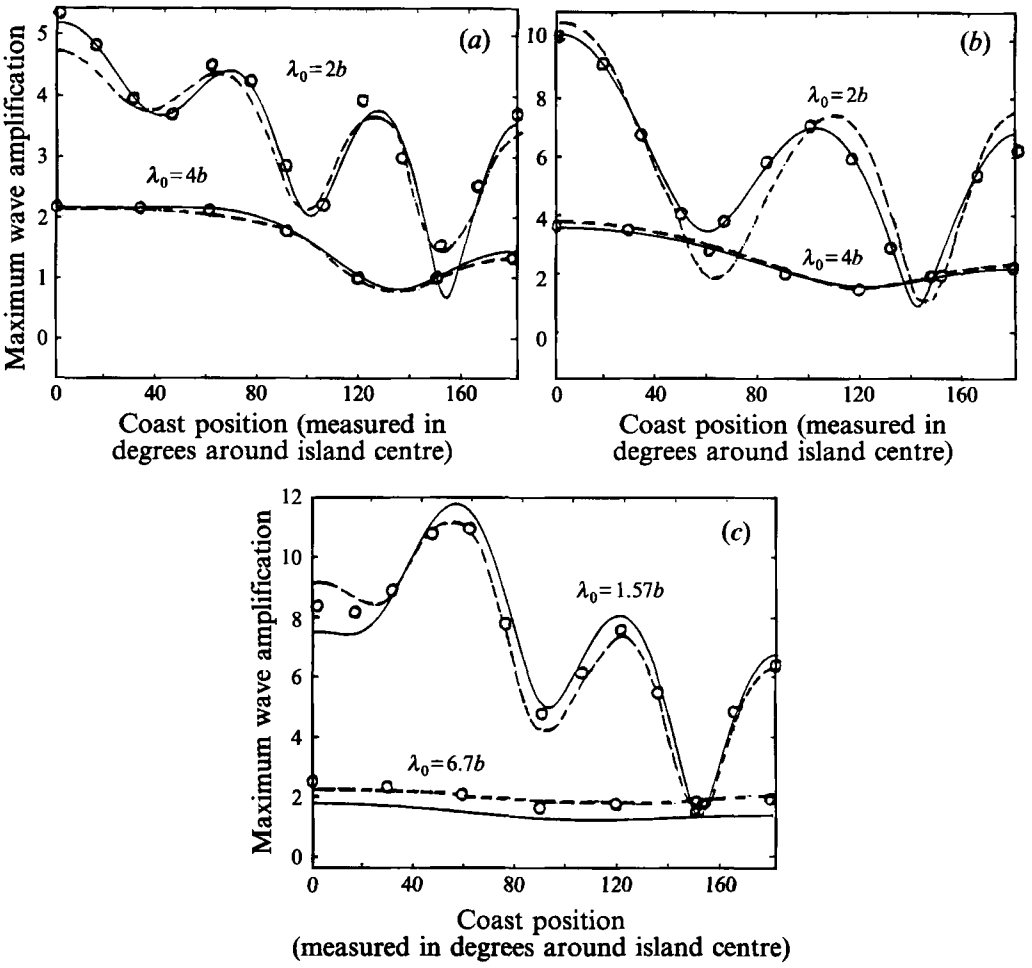

FIGURE 2. Comparison between the analytical solution presented in this paper (solid line), Smith & Sprinks' solution (dashed line), and Lautenbacher's solution (circles). (*a*) Hawaii ($b/a = 1.67$); (*b*) Oahu ($b/a = 4$); (*c*) Small ($b/a = 4.65$).

that have been included in their calculation. Furthermore, the discrepancies between the analytical solution, Lautenbacher's solution and Smith & Sprinks' solution deteriorate as b/a is increased (figure 2*c*), suggesting that a finer discretization for a larger shelf region is needed with Lautenbacher's method and large truncation errors have been produced with Smith & Sprinks' method (actually, they have pointed out the asymptotic series might converge so slowly that its applicability might be restricted to a small distance from the coastline).

A detailed view of the analytical solution for Small Island is presented in figures 3 and 4, in which the equal-value contours of relative wave amplitudes and the phase of η (equivalent to wave fronts) are shown respectively. Wave amplitudes are found to be small except in the vicinity of the coastline (see figure 3), suggesting that there is a concentration of wave energy, especially at the front face of the island. It is possible that waves have been *almost* trapped near the coastline of the island in this case (Longuet-Higgins 1967).

To examine wave amplifications in the shelf region as a response to the wave frequency, we followed Smith & Sprinks (1975) to plot in figure 5 the response curve

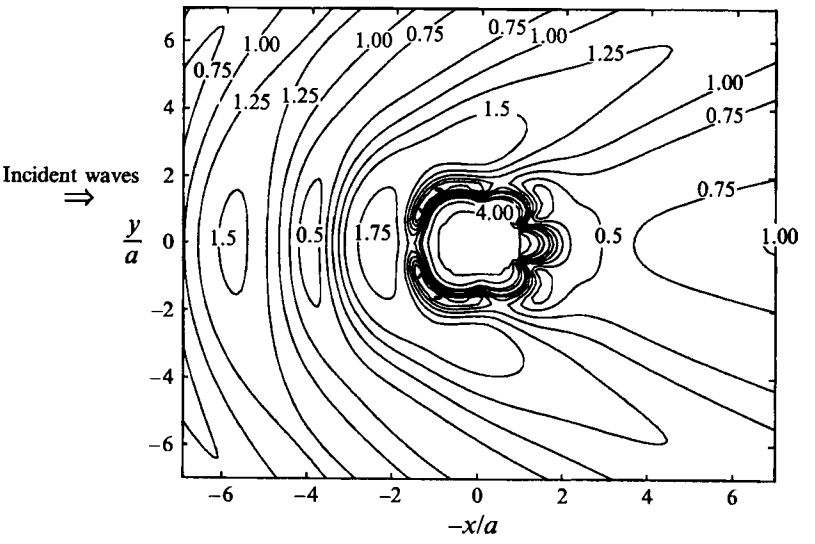

FIGURE 3. Equal-value contour lines of relative amplitudes around a conical island ($b/a = 4.65, \lambda_0 = 1.57b$).

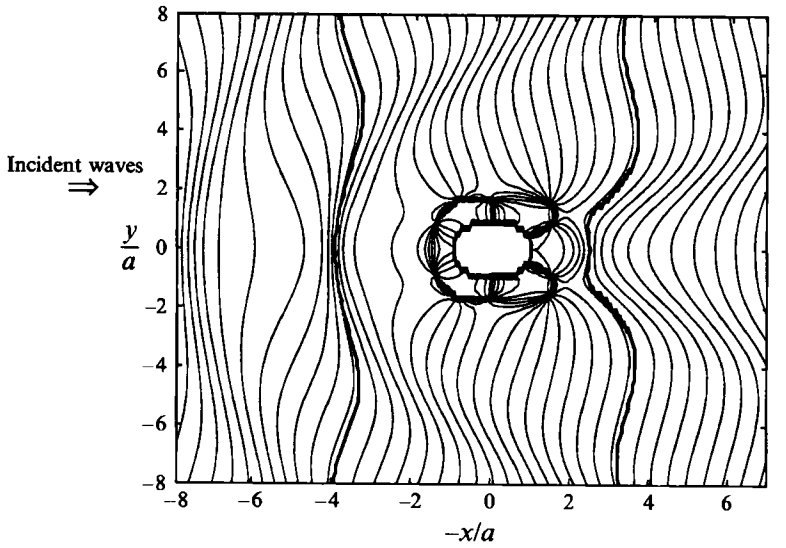

FIGURE 4. Equal-value contour lines of phase of η (i.e. wave front) around a conical island ($b/a = 4.65, \lambda_0 = 1.57b$).

of $|A_n|$ as a function of the dimensionless wave frequency $\omega(a/g)^{1/2}$ for the first five modes ($n = 0$–4) for the same conical island used for their figure 5. One can clearly see how large the wave amplitude can be built up at a certain frequency, especially for higher modes, due to the mechanism of refractive focusing (Eckart 1950). Also shown in this figure are the resonance frequencies predicted for the edge waves with zero seaward mode number using a short-wave asymptotic solution by Smith (1974). On comparing figure 5 with figure 5 in Smith & Sprinks' (1975) paper, it was found that the resonance frequencies predicted by the long-wave equation are very close to those by the mild-slope equation, though the values of $|A_n|$ may differ. For the particular

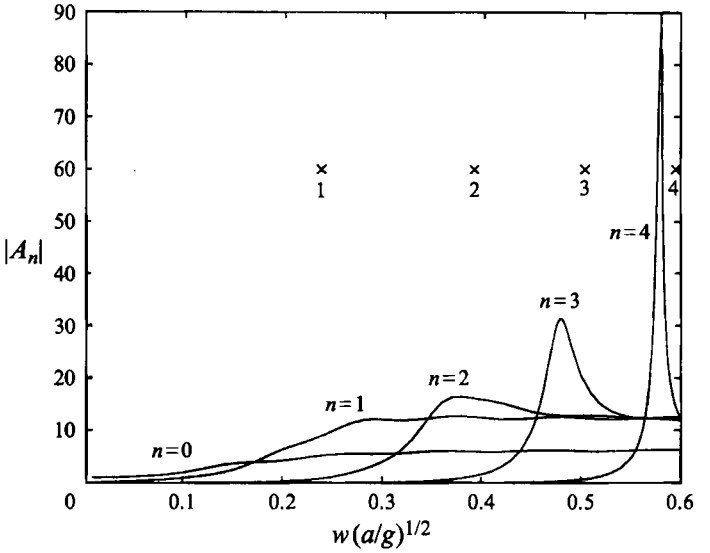

FIGURE 5. Frequency dependence of the amplitude factors A_n for a conical island used in an experiment by Barnard *et al.* ($\gamma = 0.1, b/a = 20$); ×, resonance frequencies for edge waves obtained by Smith (1974).

geometry used for their figure 5, the first significant resonance (say, mode 3) occurs at short wavelength for which the long-wave approximation is violated, as pointed out by Smith & Sprinks (1975); however, exactly the same patterns of resonances as in figure 5 can occur with long waves over shallower water since the constant depth h_0 and the wave period T can be varied in a certain way without any effects on the final solution, as stated before.

It should be emphasized here that different boundary conditions with or without a vertical wall located at the coast result in quite different responses near the coast. For the geometries studied by Homma (1950), Vastano & Reid (1966), Zhu & Zhang (1994) and others, the islands were surrounded by a vertical wall where the water depth is non-zero. Consequently, in the case studied by them, the normal velocity must vanish at the coastline, whereas in the case studied in this section, there is a large gradient of wave amplitudes in the vicinity of the island (cf. figure 6*b*). Hence one expects much larger wave amplifications and a large normal velocity (which has been shown to be proportional to the wave run-up at the coastline) near the island for boundary conditions of sloping beach type. Such an expectation is indeed confirmed by figure 6(*a*, *b*), in which the analytical solution for Oahu with the assumption of zero water depth at the coastline is compared with that for a similar island presented by Zhu & Zhang (1994) with the same values of b/a and λ_0/b but with the assumption of non-zero water depth at the coastline. Wave amplitudes obtained from the boundary condition of sloping beach type are generally well above those from the boundary condition of vertical wall type in the neighbourhood of the island. By virtue of the linearized Lagrange equation, the dynamic pressure is proportional to the water elevation; therefore the above discussion suggests that a conical island without a vertical wall located at the coastline usually bears a much larger maximum dynamic pressure.

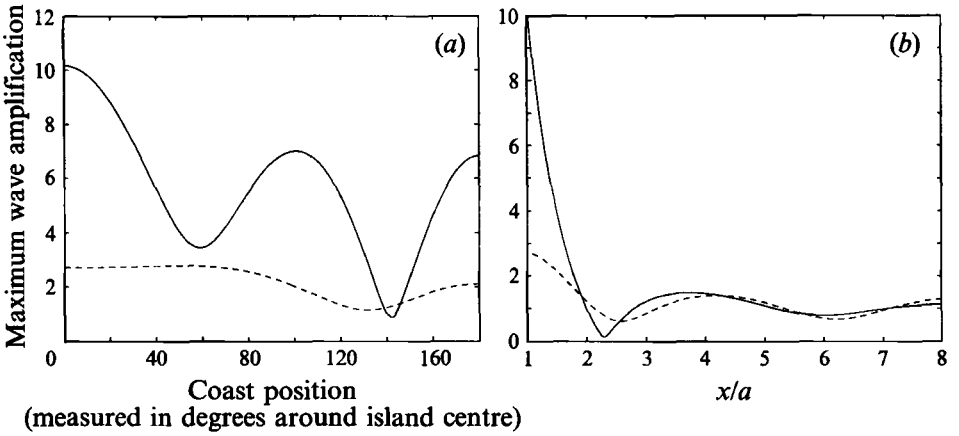

FIGURE 6. Comparison of relative amplitudes between a conical island (solid line) and an island–shelf system (dashed line) ($b/a = 4, \lambda_0/b = 2$): (*a*) along the shoreline of the island; (*b*) along the direction of incident waves ($\theta = 0$).

4. Refraction of plane long waves by a paraboloidal shoal

Refraction of plane waves over a paraboloidal shoal (figure 7) has been studied either numerically or experimentally by many researchers (Berkhoff 1972; Fokstra & Berkhoff 1977; Radder 1979; Panchang, Cushman-Roisin & Pearce 1988; Zhu 1993). However, the analytical solutions have never been presented before; numerical results were often compared with each other. Therefore this problem is ideal to be our second example.

Consider a train of plane long waves propagating along the x-direction and being refracted by the shoal. Owing to the shoaling of the water depth towards the centre of the shoal, the waves may be greatly amplified. At first glance, it seems that no diffraction is present, but the results from ray theory (geometric optics) reveals that wave rays converge to form caustics in the lee region of the shoal where diffraction effects are significant.

In this problem, the radius of the shoal, a, is chosen as the characteristic lengthscale, L_s. In the region with variable water depth $r \leqslant 1$, we have $h = h_m(1+\beta r^2)$ with $\beta = (h_0 - h_m)/h_m$, and therefore (5) reads

$$r^2(1+\beta r^2)R_n'' + (3\beta r^3 + r)R_n' + (\nu^2 r^2 - \beta n^2 r^2 - n^2)R_n = 0, \tag{26}$$

or

$$t^2(t+1)\frac{\mathrm{d}^2 R_n}{\mathrm{d}t^2} + t(2t+1)\frac{\mathrm{d}R_n}{\mathrm{d}t} + \left(\frac{\nu^2 t}{4\beta} - \tfrac{1}{4}n^2 t - \tfrac{1}{4}n^2\right)R_n = 0, \tag{27}$$

where $t = \beta r^2$, $\nu^2 = (1+\beta)k_0^2$, and k_0 is the dimensionless wavenumber in the constant-depth region. Unlike the conical island discussed in the previous section, there is no boundary condition imposed in the region of variable water depth. Instead, the condition that water elevation must be finite at the origin must be imposed. To readily make use of this condition, the origin, which is a regular singular point of (26) (or (27)), is chosen as the expansion point. From Frobenius' theory, the series solution converges for $|t| < 1$, which may or may not include the domain of concern (i.e. the region of variable water depth $0 \leqslant t \leqslant \beta$). However, we can employ two 'shift' and one 'mapping' transformations to 'move' the domain of interest into the convergent region of the series solution. Upon successive transformations with respect to the independent variable t:

$$u = 1+t, \quad s = 1/u, \quad v = 1-s, \tag{28}$$

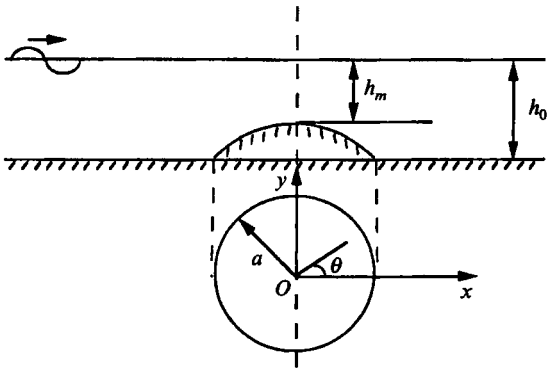

FIGURE 7. A definition sketch: refraction of plane waves over a parabolic shoal.

the domain of interest is mapped successively to: $1 \leqslant u \leqslant 1+\beta$, $1/(1+\beta) \leqslant s \leqslant 1$, $0 \leqslant v \leqslant \beta/(1+\beta)\,(<1)$, and (27) becomes

$$v^2(1-v)^2\frac{\mathrm{d}^2R_n}{\mathrm{d}v^2}+v(1-v)^2\frac{\mathrm{d}R_n}{\mathrm{d}v}+(\nu^2v/4\beta-\tfrac{1}{4}n^2)\,R_n=0. \tag{29}$$

The final independent variable v has a relation with the original independent variable r

$$v=\frac{\beta r^2}{1+\beta r^2}, \tag{30}$$

and therefore $r=0$ has been mapped onto $v=0$, which is still a regular singular point of (29). Thus Frobenius' series solution of the form

$$R_n(v)=\sum_{m=0}^{\infty}a_{m,n}\,v^{m+c} \tag{31}$$

with $a_{0,n}$ being unity, converges for $|v|<1$, which encompasses the mapped domain of interest ($v\in(0,\beta(1+\beta)^{-1})$).

Upon substituting (31) into (29) and collecting terms of the same order of v, one obtains

$$c=\pm\tfrac{1}{2}n, \tag{32}$$

$$a_{1,n}=(2c^2-\nu^2/4\beta)\,[(c+1)^2-\tfrac{1}{4}n^2]^{-1}, \tag{33}$$

$$a_{m+2,n}=\frac{[2(m+1+c)^2-\nu^2/4\beta]\,a_{m+1,n}-(m+c)^2a_{m,n}}{(m+2+c)^2-\tfrac{1}{4}n^2}, \quad m=0,1,2,\ldots. \tag{34}$$

Since the two roots of the indicial equation ($c=\pm\frac{1}{2}n$) differ by an integer, the corresponding two particular solutions become linearly dependent. However, it can be proved (Spiegel 1981) that another independent particular solution $[\partial R_n(v,c)/\partial c]_{c=n/2}$ contains $\ln v$ which is singular at $v=0$. Therefore the general solution in this region is just

$$R_n(r)=A_n\sum_{m=0}^{\infty}a_{m,n}\left(\frac{\beta r^2}{1+\beta r^2}\right)^{m+n/2}\equiv A_n\,\bar{R}_n(r), \tag{35}$$

with $c=\frac{1}{2}n$, and the water elevation

$$\eta_1(r,\theta)=\sum_{n=0}^{\infty}A_n\,\bar{R}_n(r)\cos n\theta, \tag{36}$$

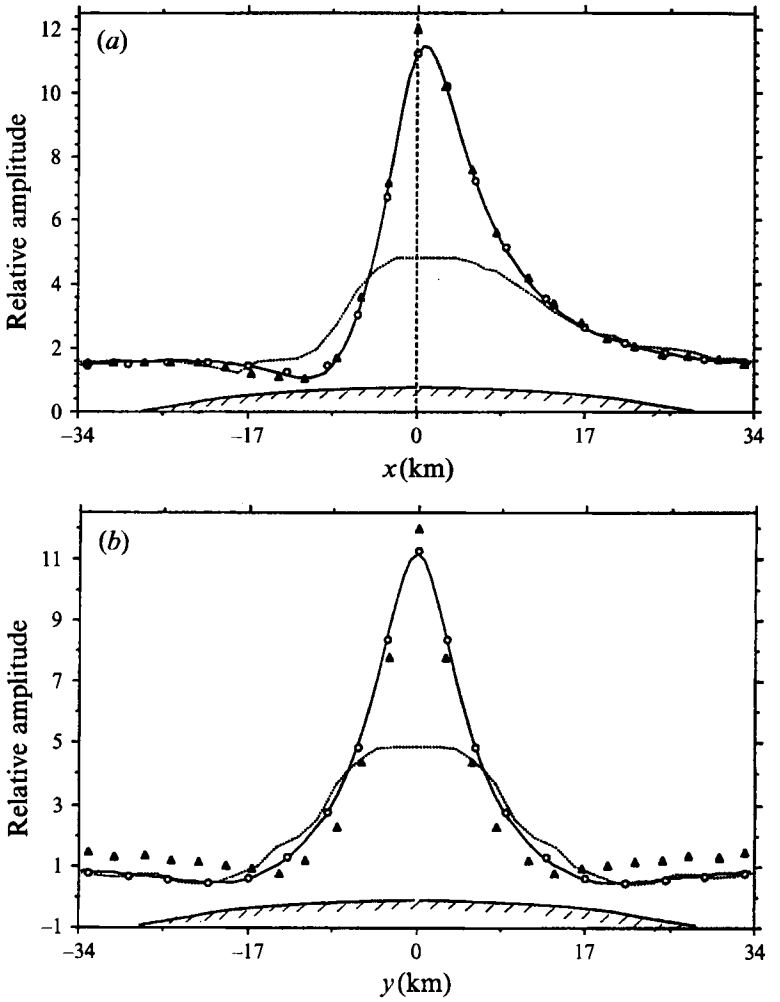

FIGURE 8. Comparison of relative wave amplitudes between the analytical solution in this paper (solid line), and the solutions of Berkhoff (dashed line), Bettess & Zienkiewitz (triangles), and Zhu (circles) for a paraboloidal shoal with $\beta = 79, \lambda_0/a = 4.32$. (*a*) $y = 0$; (*b*) $x = 0$.

in which the coefficients A_n can be determined by matching the solution in this region with that in the region of constant water depth. Since now the incident waves travel along the x-direction instead of the negative x-direction, the general solution in the constant-depth region can be written as

$$\eta_2(r,\theta) = \eta_2^I + \eta_2^S = \sum_{n=0}^{\infty} [\mathrm{i}^n \epsilon_n J_n(k_0 r) + C_n H_n^{(1)}(k_0 r)] \cos n\theta,$$

where $H_n^{(1)}$ denotes the Hankel function of the first kind of order n. The coefficients A_n and C_n are then determined by matching the solutions in the two regions as

$$A_n = -2\epsilon_n \mathrm{i}^{n+1}/\pi \Delta, \tag{37}$$

$$C_n = \Delta_1/\Delta, \tag{38}$$

$$\Delta = \begin{vmatrix} \bar{R}_n(1) & -H_n^{(1)}(k_0) \\ \bar{R}_n'(1) & -k_0 H_n^{(1)'}(k_0) \end{vmatrix}, \quad \Delta_1 = \mathrm{i}^n \epsilon_n \begin{vmatrix} \bar{R}_n(1) & J_n(k_0) \\ \bar{R}_n'(1) & k_0 J_n'(k_0) \end{vmatrix},$$

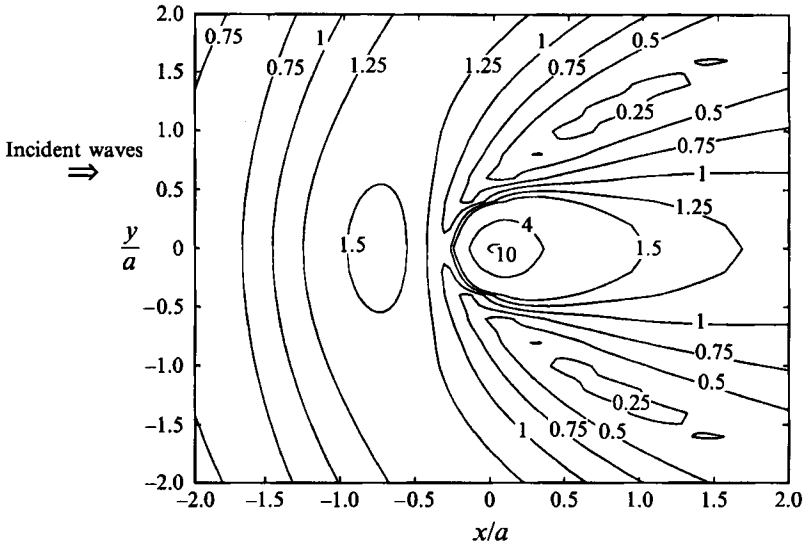

FIGURE 9. Equal-value contour lines of relative amplitudes around a paraboloidal shoal ($\beta = 79, \lambda_0/a = 4.32$).

where $\bar{R}_n(r)$ has been given in (35) and the prime denotes derivatives with respect to the arguments. Consequently, the motion at the origin is simply

$$[\zeta_1]_{r=0} = A_0 \exp(-i\omega\tau). \tag{39}$$

Similar to the case studied in the previous section, the analytical solution is expressed in terms of a geometric parameter $\beta(=(h_0-h_m)/h_m)$ and a dimensionless wavelength λ_0/a. The constant water depth h_0 is a free parameter.

Numerical solutions for this problem have been presented by Berkhoff (1972) and Bettess & Zienkiewitz (1977). However, there is a large discrepancy between their solutions, especially near the centre of the shoal. Recently, the same problem was also solved with the dual-reciprocity boundary element method by Zhu (1993), who found his solution was in close agreement with Bettess & Zienkiewitz's solution near the centre of the shoal but in close agreement with Berkhoff's solution near the edge of the shoal. Having obtained the analytical solution, we can discuss the accuracy associated with these numerical solutions.

Dimensionless wave amplitudes calculated from different models along two sections $y = 0$ and $x = 0$ across the shoal are shown in figures 8(*a*) and 8(*b*) respectively. From these figures, it can be seen that Zhu's solution is in excellent agreement with the analytical solution presented in this paper; Bettess & Zienkiewitz's solution is close to the analytical solution along the line of symmetry ($y = 0$) but is less accurate along the direction perpendicular to the line of symmetry, especially near the edge of the shoal. For Berkhoff's solution, substantial deviation from the analytical solution near the centre of the shoal is observed. Such a large discrepancy may be due to the relatively coarse grids used in his calculation.

To give a closer view of the entire wave field, the contour lines of the dimensionless wave amplitude and the phase of η (wave fronts) are presented in figures 9 and 10 respectively. A large gradient of wave amplitude variation is observed at the front face of the shoal whereas the largest amplitude is found in the lee region, suggesting strong diffraction effects there. In the same time, wave fronts are refracted towards the centre of the shoal, as shown in figure 10.

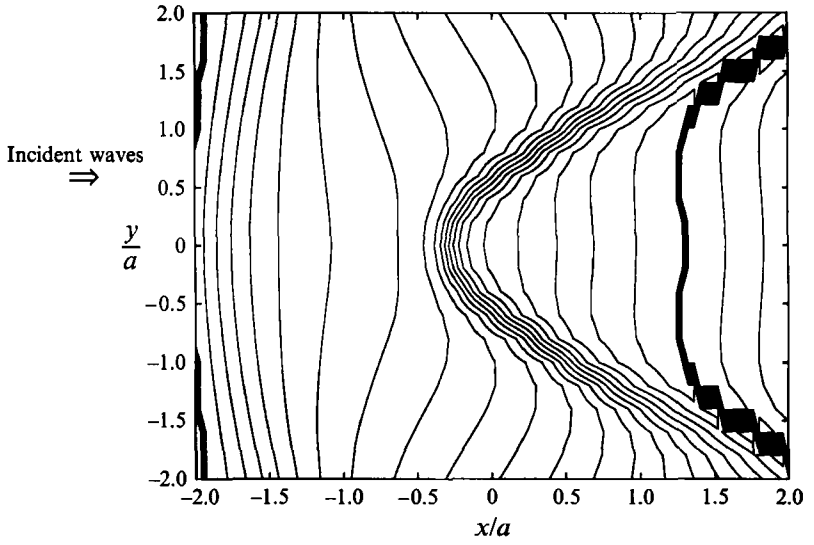

FIGURE 10. Equal-value contour lines of phase of η (i.e. wave front) around the paraboloidal shoal ($\beta = 79, \lambda_0/a = 4.32$).

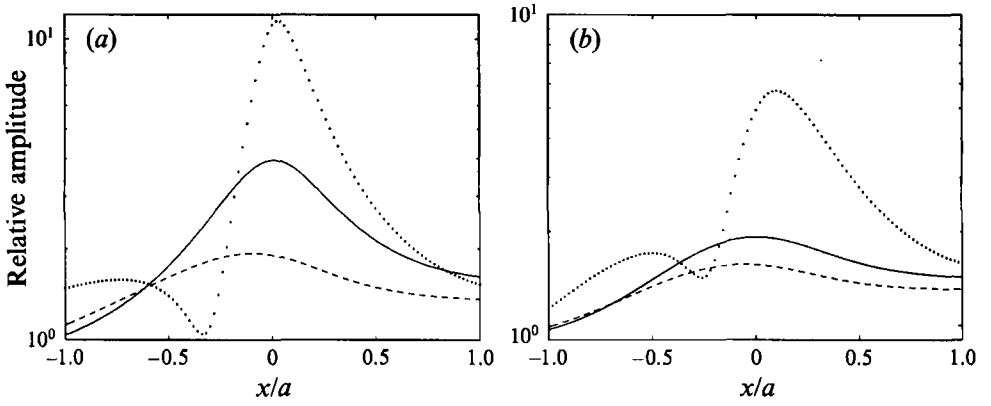

FIGURE 11. Response over the shoal for different values of β and λ_0/a. (*a*) $\lambda_0/a = 4.32$, $\beta = 4$ (dashed line), $\beta = 15$ (solid line), $\beta = 79$ (dotted line); (*b*) $\lambda_0/a = 3.49$, $\beta = 1$ (dashed line), $\beta = 2.5$ (solid line), $\beta = 20$ (dotted line).

The concentration of wave energy in a certain region and the large response in the lee region in this case can be attributed to the combined refraction and diffraction effects. For a shoal with small β (i.e. a flatter shoal), both the refraction and diffraction are weak and thus one expects an almost even distribution of wave heights across the shoal. On the other hand, for a rather peaked shoal (such as the example shown above) there is more refractive focusing, as can be demonstrated with the conventional ray theory. Furthermore, owing to a more rapid variation of seabed, diffraction effects also become stronger on the lee side of the shoal (Mei 1989). These possibilities are confirmed by figure 11 (*a*, *b*), in which the wave amplitudes over the shoal along the line of symmetry are shown for different values of β and λ_0/a. For small β, the maximum wave amplitude occurs at the front face of the shoal. As β is increased, the location of the maximum wave amplitude moves towards the centre of the shoal, passes it, and

then continues to move into the lee region. Associated with this process is a gradual concentration of wave energy into a region where the maximum wave amplitude occurs, as a consequence of refractive focusing. Furthermore, comparing figure 11(*a*) with 11(*b*) reveals that diffraction effects are more significant for waves of shorter period.

5. Conclusions

In this paper, a widely applicable approach to solving analytically long-wave propagation over waters of variable depth has been demonstrated using two combined refraction and diffraction problems as examples. Generally speaking, a Frobenius series solution can be constructed in the region of variable water depth, even for a more general bottom topography, as long as it is axisymmetric. However, appropriate transformations may need to be constructed so that the convergent region of the series lies within the region of interest. Such transformations are the key to a successful solution.

An analytical solution for long waves scattered by a conical island standing in an open sea of constant depth was presented in §3. After comparing the results obtained with and without a vertical wall located at the coastline, we found an island without a vertical wall located at the coastline induced much stronger wave amplifications near the coastline; waves are more trapped there.

Combined refraction and diffraction effects were discussed with our second analytical solution for long-wave propagation over a submerged paraboloidal shoal presented in §4. The effects were found to be dependent on both the wave frequency and the amount of protrusion of the shoal; as the shoal becomes more and more protruded, the location of the maximum wave amplitude moves towards the lee region of the shoal, and at the same time, there is a gradual concentration of wave energy into a region where the maximum wave amplitude occurs, as a consequence of refractive focusing. Furthermore, these phenomena become more obvious for shorter-period waves.

We have also taken advantage of the newly derived analytical solutions in discussing the accuracy of several previously presented numerical solutions in the literature. The results of our comparison can be summarized as follows.

(i) A comparison of two numerical solutions due to Lutenbacher (1972) and Smith & Sprinks (1975) for long waves scattered by a conical island with the newly derived analytical solution, showed that the results from both numerical solutions are not very satisfactory especially for waves of comparatively short periods or for an island with a large shelf region.

(ii) For long waves over a paraboloidal shoal, there are several numerical solutions which are quite different from each other. The dispute on which solution is the most accurate one was finally terminated by the newly obtained analytical solution. We concluded that Zhu's (1993) solution is the most accurate one; Bettess & Zienkiewitz's (1977) solution is reasonably close to the analytical solution except in certain regions near the edge of the shoal, and Berkhoff's (1972) solution is erroneous near the centre of the shoal.

The authors wish to thank Mr Pornchai Satravaha and Mr Peter Tritscher for their help in drawing figure 2. Originally, owing to the formidable computational effort required in calculating the numerical results for the second analytical solution in this paper, access to a supercomputer was kindly provided by the Australian Institute of

Nuclear Science and Engineering (AINSE) under the AINSE Grant 93/148. Although the computational effort had been greatly relieved once the new form of the analytical solution (presented in this paper) was obtained and a supercomputer was no longer required to calculate the results presented in §4, the AINSE's generous support is still gratefully acknowledged.

REFERENCES

BERKHOFF, J. C. W. 1972 Computation of combined refraction-diffraction. In *13th Intl Conf. Coastal Engng*, Vol. 1, pp. 471–490.

BETTESS, P. & ZIENKIEWICZ, O. C. 1977 Diffraction and refraction of surface waves using finite and infinite elements. *Intl J. Num. Meth. Engng* **11**, 1271–1290.

CHRISTIANSEN, P. L. 1977 Diffraction of gravity waves by ray methods. In *Waves on Water of Variable Depth* (ed. D. G. Provis & R. Radok). Lecture Notes in Physics, vol. 64. Springer.

ECKART, C. 1950 The ray particle analogy. *J. Mar. Res.* **9**, 139–144.

ECKART, C. 1951 Surface waves on water of variable depth. *Scripps Inst. Oceanogr., Lecture Notes, Fall Semester 1950–51, Ref.* 51-12, *Wave Rep.* 100.

FLOKSTRA, C. & BERKHOFF, J. C. W. 1977 Propagation of short waves over a circular shoal. *Delft Hydraulics Lab. Rep.* W. 154-V (in Dutch).

HOMMA, S. 1950 On the behaviour of seismic sea waves around circular island. *Geophys. Mag.* **XXI**, 199–208.

ITO, Y. & TANIMOTO, K. 1972 A method of numerical analysis of wave propagation – application to wave diffraction and refraction. In *13th Coastal Engng Conf.*, Vol. 1, pp. 503–522.

KIRBY, J. T. & DALRYMPLE, R. A. 1983 A parabolic equation for the combined refraction-diffraction of Stokes waves by mildly varying topography. *J. Fluid Mech.* **136**, 453–466.

LAUTENBACHER, C. C. 1970 Gravity wave refraction by islands. *J. Fluid Mech.* **41**, 655–672.

LONGUET-HIGGINS, M. S. 1967 On the trapping of wave energy round islands. *J. Fluid Mech.* **29**, 781–821.

MACCAMY, R. C. & FUCHS, R. A. 1954 Wave forces on piles: a diffraction theory. *US Army Corps of Engineering, Beach Erosion Board, Washington, DC, Tech. Mem.* 69.

MEI, C. C. 1989 *The Applied Dynamics of Ocean Surface Waves*. World Scientific.

PANCHANG, V. G., CUSHMAN-ROISIN, B. & PEARCE, B. R. 1988 Combined refraction–diffraction of short-waves in large coastal regions. *Coastal Engng* **12**, 133–156.

PANCHANG, V. G. & KOPRIVA, D. A. 1989 Solution of two-dimensional water-wave propagation problems by Chebyshev collocation. *Math. Comput. Modelling* **12**, 625–640.

RADDER, A. C. 1979 On the parabolic equation method for water-wave propagation. *J. Fluid Mech.* **95**, 159–176.

SARPKAYA, T. & ISAACSON, M. 1981 *Mechanics of Wave Force on Offshore structures*. Van Nostrand Reinhold.

SHEN, M. C. & MEYER, R. E. 1968 Spectra of water waves in channels and around islands. *Phys. Fluids* **11**, 2289–2304.

SMITH, R. 1974 Edge waves on a beach of mild slope. *Q. J. Mech. Appl. Maths* **27**, 102–110.

SMITH, R. & SPRINKS, T. 1975 Scattering of surface waves by a conical island. *J. Fluid Mech.* **72**, 373–384.

SPIEGEL, M. R. 1981 *Applied Differential Equations*. Prentice-Hall.

VASTANO, A. C. & REID, R. O. 1966 A numerical study of the tsunami response at an island. *Texas A&M University Project* 471, *Ref.* 66-26T.

ZHU, S.-P. 1993 A new DRBEM model for wave refraction and diffraction. *Engng Ana. Boundary Elements* (in the press).

ZHU, S.-P. & ZHANG, Y.-L. 1994 Scattering of long waves around a circular island mounted on a conical shoal. *J. Mar. Res.* (submitted).